Biophysical Journal Volume 68 March 1995 729–738

Calculations of the Electrostatic Potential Adjacent to Model Phospholipid Bilayers

Robert M. Peitzsch,* Moisés Eisenberg,‡ Kim A. Sharp,§ and Stuart McLaughlin*

*Department of Physiology and Biophysics and ‡Department of Pharmacological Sciences, HSC, SUNY Stony Brook, Stony Brook, New York 11794; §Johnson Research Foundation, Department of Biochemistry and Biophysics, University of Pennsylvania, Philadelphia, Pennsylvania 19104 USA

ABSTRACT We used the nonlinear Poisson-Boltzmann equation to calculate electrostatic potentials in the aqueous phase adjacent to model phospholipid bilayers containing mixtures of zwitterionic lipids (phosphatidylcholine) and acidic lipids (phosphatidylserine or phosphatidylglycerol). The aqueous phase (relative permittivity, $\epsilon_r = 80$) contains 0.1 M monovalent salt. When the bilayers contain <11% acidic lipid, the −25 mV equipotential surfaces are discrete domes centered over the negatively charged lipids and are approximately twice the value calculated using Debye-Hückel theory. When the bilayers contain >25% acidic lipid, the −25 mV equipotential profiles are essentially flat and agree well with the values calculated using Gouy-Chapman theory. When the bilayers contain 100% acidic lipid, all of the equipotential surfaces are flat and agree with Gouy-Chapman predictions (including the −100 mV surface, which is located only 1 Å from the outermost atoms). Even our model bilayers are not simple systems: the charge on each lipid is distributed over several atoms, these partial charges are non-coplanar, there is a 2 Å ion-exclusion region ($\epsilon_r = 80$) adjacent to the polar headgroups, and the molecular surface is rough. We investigated the effect of these four factors using smooth (or bumpy) $\epsilon_r = 2$ slabs with embedded point charges: these factors had only minor effects on the potential in the aqueous phase.

INTRODUCTION

We report here a calculation of the electrostatic potential in the aqueous phase adjacent to a model phospholipid bilayer formed from a mixture of zwitterionic and acidic lipids. Several groups have reviewed the problem of calculating the electrostatic potential adjacent to macromolecules (Matthew, 1985; Honig et al., 1986; Davis and McCammon, 1990; Sharp and Honig, 1990; Sharp, 1994) and membranes (McLaughlin, 1977, 1989; Cevc and Marsh, 1987; Cevc, 1990; Israelachvili, 1991).

The simplest approach to this problem is to use the mean-field Gouy-Chapman theory and calculate the average electrostatic potential from the one-dimensional Poisson-Boltzmann (PB) equation. This approach makes a number of simplifying assumptions, including assuming the charges on the lipids are smeared uniformly over a planar surface, but it provides a surprisingly adequate description of many electrostatic phenomena. For example, the smeared charge Gouy-Chapman theory has been applied successfully to explain the electrostatic repulsion between charged bilayers (Marra, 1986; Evans and Parsegian, 1986), the ζ potential of phospholipid vesicles (McLaughlin and Harary, 1976; Winiski et al., 1986), how salt affects the surface potential above phospholipid monolayers (McDonald and Bangham, 1972; Lakhdar-Ghazal et al., 1983), and how the potential adjacent to a bilayer membrane depends on distance from the surface (Winiski et al., 1986, 1988; Langner et al., 1990; Kraayenhof et al., 1993). Other phenomena, however, require a more realistic treatment of the potential. Specifically, basic peptides (de Kruijff et al., 1985; Kim et al., 1991; Mosior and McLaughlin, 1992a, b) and basic regions of proteins such as myosin I (Adams and Pollard, 1989; Pollard et al., 1991), myosin II (Li et al., 1994), protein kinase C (Mosior and McLaughlin, 1991; Newton, 1993), $p21^{K\text{-}ras(B)}$ (Hancock et al., 1990; Magee et al., 1992), myristoylated alanine-rich C kinase substrate (Taniguchi and Manenti, 1993; Kim et al., 1994), and $pp60^{src}$ (Buser et al., 1994) adsorb to acidic lipids in membranes. We have shown that this binding can be described, to a first approximation, by combining the Gouy-Chapman and mass-action equations (Kim et al., 1991; Mosior and McLaughlin, 1992b). This simplified description includes assumptions that both peptides and lipids are dimensionless points, that the discrete pair-wise electrostatic attraction between individual basic residues and acidic lipids can be ignored, and that the charges on the lipids are smeared uniformly over a planar interface. These assumptions must be abandoned to obtain a more realistic theoretical model of electrostatic lipid-protein interactions.

Several groups have made important contributions to the discreteness-of-charge problem, but most of these approaches are specifically directed to the potential at a metal-water surface (e.g., Grahame, 1958; Levine, 1971). A number of investigators (Nelson and McQuarrie, 1975; Sauve and Ohki, 1979; Mathias et al., 1992; Arakelian et al., 1993; Forsten et al., 1994) have calculated potentials produced by

Received for publication 21 July 1994 and in final form 15 November 1994.

Address reprint requests to Dr. Stuart G. McLaughlin, Department of Physiology/Biophysics, SUNY Health Science Center–Stony Brook, Stony Brook, NY 11794-8661. Tel.: 516-444-3615; Fax: 516-444-3432; E-mail: SMCL@EPO.SOM.SUNYSB.EDU.

Abbreviations used in this article: ϵ_r, relative permittivity; PC, 1-palmitoyl-2-oleoyl-*sn*-glycero-3-phosphocholine; PG, 1-palmitoyl-2-oleoyl-*sn*-glycero-3-phosphoglycerol; PS, 1-palmitoyl-2-oleoyl-*sn*-glycero-3-phosphoserine; e, electronic charge; ϵ_0, permittivity of free space; ϕ, electrostatic potential.

0006-3495/95/03/729/10 $2.00

fixed discrete charges located within a planar slab of low relative permittivity (ϵ_r) using the PB equation.

Our approach is to construct a molecular model of a phospholipid bilayer containing a mixture of acidic and zwitterionic lipids, then calculate the potential in the aqueous phase adjacent to the bilayer using the nonlinear PB equation. The structure of phospholipids in bilayers is now understood reasonably well. There is good evidence that the glycerol backbone is essentially perpendicular to the plane of the membrane (Pearson and Pascher, 1979) and that the polar headgroups are approximately parallel to the surface (Büldt et al., 1979; Hauser et al., 1981; Seelig et al., 1987; Akutsu and Nagamori, 1991; Wiener and White, 1992). For lipids containing unsaturated chains, the area per lipid is 65–70 Å^2 (Shipley, 1973; Rand, 1981; McIntosh et al., 1989). The charge distribution within phospholipids has been calculated by several groups (Peinel, 1975; Charifson et al., 1990; Stouch and Williams, 1992) and the ϵ_r in the interior of the bilayer is known to be about 2 from a combination of capacitance and thickness measurements (Fettiplace et al., 1971; Dilger and Benz, 1985). The available evidence suggests the water in the diffuse double layer adjacent to the bilayer has an effective dielectric constant equal to its bulk value (Marra, 1986; Langner et al., 1990; Kraayenhof et al., 1993). One problem is that we have little information about the dielectric constant of the polar headgroup region (Ashcroft et al., 1981). (Calculations of the potential within this region also require assumptions about the orientation of water molecules; several groups have investigated the dipole potential produced by these oriented waters (Simon and McIntosh, 1989; Zheng and Vanderkooi, 1992; Alper et al., 1993; Wilson and Pohorille, 1994).) We partially finesse this problem by calculating only the electrostatic potential in the aqueous phase *outside* the polar headgroup region. This potential does not depend greatly on the assumptions we make about the dielectric constant of the aqueous ion-exclusion layer or the partial charges we assign to the atoms in the phospholipid headgroups. Specifically, we assume water can penetrate into the polar region, and the volume it occupies has $\epsilon_r = 80$, while the volume occupied by the headgroups themselves has an $\epsilon_r = 2$. Ions are not allowed to penetrate the headgroup region: they are restricted to a region outside a 2 Å thick "ion-exclusion layer" that extends from the van der Waals envelope of the headgroup atoms. We assume the aqueous phase adjacent to the membrane has an $\epsilon_r = 80$ and make all other conventional assumptions inherent in the simplest use of the PB equation. Specifically, the potential of mean force is replaced by the mean electrostatic potential in the PB equation and all ion-ion correlations in the double layer are ignored. In the conventional "restricted primitive" model of the electrolyte solution we use, ions are dimensionless point charges and water is a structureless medium. We then solve the three-dimensional PB equation as described below to calculate the potential adjacent to membranes formed from either zwitterionic (PC) or acidic (PS and PG) lipids, or from mixtures of these lipids.

Even with the above assumptions, our model of the bilayer-water surface is not a simple system: 1) the charges on the lipids are distributed over adjacent atoms, 2) these partial charges are not coplanar, 3) there is a 2 Å, $\epsilon_r = 80$, ion-exclusion layer adjacent to the polar headgroups, and 4) the surface of the bilayer is not a plane. We considered simple models of point charges embedded in a planar (or bumpy) low-dielectric, ion-impenetrable slab to investigate the importance of each of these phenomena.

MATERIALS AND METHODS

Bilayer model

We built all-atom molecular models of PC, PS, and PG using Biograph (Biodesigns Inc., Pasadena, CA) version 2.11 running on an Alliant FX-1 (Alliant Computer Systems Corp., Littleton, MA) with an Evans & Sutherland PS 390 graphics workstation (Evans and Sutherland Computer Corp., Salt Lake City, UT) and constructed bilayers with these model lipids. We used the coordinates available in the program's library. Subsequently, we rotated several bonds to obtain a conformation that satisfied the following criteria: 1) the glycerol backbone would be oriented in the same direction as the fatty acid chains, perpendicular to the plane of the bilayer, 2) the polar headgroup would lie approximately parallel to the membrane's surface, and 3) all saturated fatty acid chain bonds would be in the *trans* conformation. The glycerol backbone and headgroup orientations are based on the available experimental evidence from nuclear magnetic resonance (NMR) (Scherer and Seelig, 1987; Seelig et al., 1987), neutron and x-ray diffraction (Büldt et al., 1979; Pearson and Pascher, 1979; Hauser et al., 1981; Weiner and White, 1992), and Raman scattering (Akutsu and Nagamori, 1991) measurements. For example, the polar headgroup of our model PC has a ≈15° angle of inclination to the bilayer surface, compared with the estimate of 20° by Weiner and White (1992). Finally, 200-step energy minimization using the conjugate gradient method with a Dreiding force field was performed on each individual lipid to remove any steric hindrances or strained torsional bond angles.

We constructed 0:1, 3:1, and 8:1 PC:PS bilayers (100%, 25%, and 11% PS). We also constructed bilayers containing PG instead of PS. Fig. 1 shows the 11% PS bilayer. Each leaflet contains 192 hexagonally packed lipids, and each lipid has an area of 68 Å^2. The bilayer surface is roughly square, 130 Å × 120 Å, and the bilayers are 60 Å thick. Each leaflet's polar headgroup region is 7–8 Å thick, which leaves a 45 Å region occupied by the acyl tails. The thickness of the hydrocarbon region agrees with experimental neutron and x-ray diffraction measurements (Weiner and White, 1992), although the exact thickness chosen will not greatly affect the potential in the aqueous phase. (Chandler et al. (1965) used Gouy-Chapman theory to show that the coupling across the membrane is negligible in 0.1 M salt solutions because the capacitance of the membrane is much lower than the capacitance of the double layer. This has been confirmed by Arakelian et al. (1993) using the linearized PB equation and by Nelson et al. (1975) using the nonlinear PB equation. Under our conditions (0.1 M salt) the capacitance of the bilayer (~1 μF/cm^2) is much lower than the capacitance of the double layer (~75 μF/cm^2); thus the potential in the aqueous phase depends strongly on the concentration of acidic lipid in the adjacent leaflet but only weakly on both the charge on the other leaflet and the thickness of the membrane.)

We constructed bilayers containing acidic lipids in only one or both leaflets. The acidic lipids are distributed on a hexagonal lattice throughout each leaflet. When both leaflets contain acidic lipids, they are mirror images of each other. All lipids of the same species were oriented identically in the plane of the membrane. Other investigators have constructed similar molecular models of membranes (reviewed in Stouch, 1993).

Fig. 2 is a cartoon of a cross-section of the interface between the aqueous phase and a bilayer. The aqueous phase and salt ions are excluded from the acyl tail region of the bilayer: salt ions also are excluded from a 2 Å thick region of the aqueous phase immediately adjacent to the bilayer. Our choice

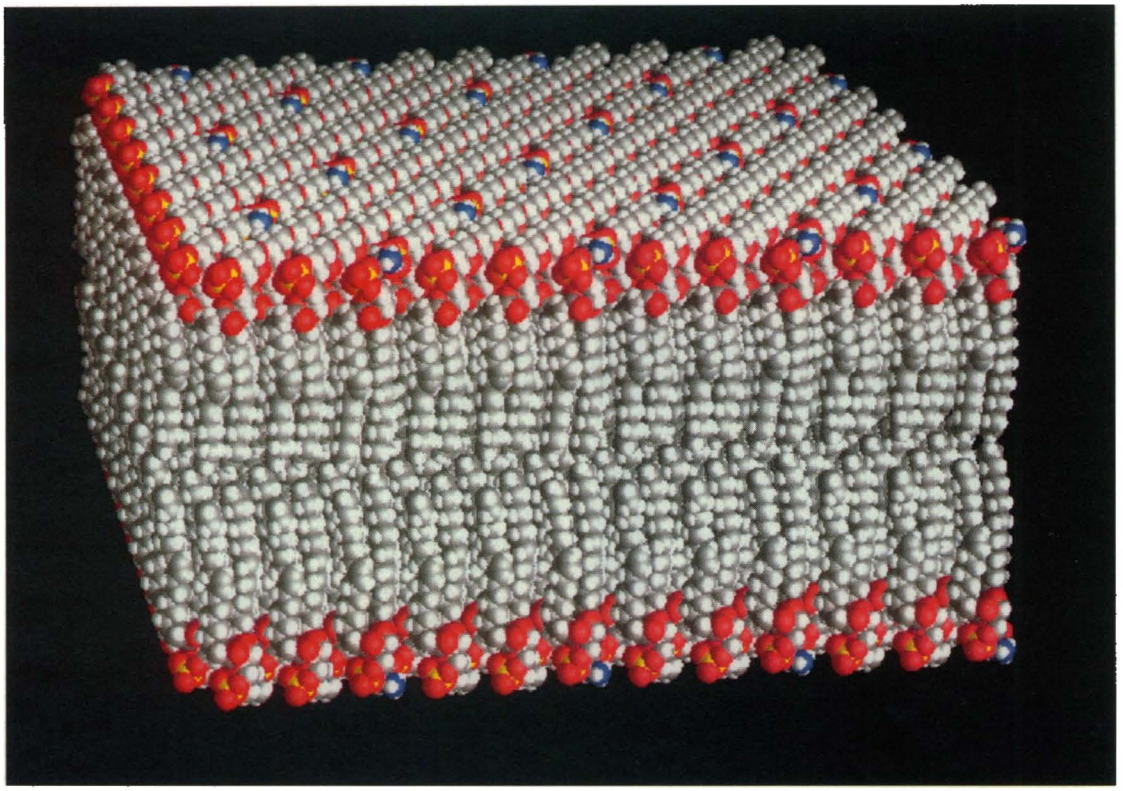

FIGURE 1 Molecular model of an 8:1 PC:PS phospholipid bilayer (11% PS). PS is easily identified by its exposed nitrogen (blue).

of 2 Å is based on the mean hydrated radii of the Na^+ and Cl^- ions obtained from experimental activity coefficients using Debye-Hückel theory (Bockris and Reddy, 1970). This salt-free aqueous phase extends into the 7–8 Å thick polar headgroup region and occupies ≈60% of this region's volume. This gives the polar headgroup region a heterogeneous dielectric constant with an average value of (0.6) (80)+(0.4) (2)≈ 50. (This side view of the lipids emphasizes the volume of the water in the polar headgroup region: a rotated view would show less water between the headgroups.)

We used the all-atom partial charges calculated by Charifson et al. (1990, Table III) with the following change: the partial charges along the fatty acid atoms below the carbonyl group were consolidated on the first carbon below the carbonyl. The rest of the fatty acid atoms were assigned a charge of 0. One reason for choosing this set of partial charges is that net charges for PS (−1) and PC (0) are correct. The most highly charged groups on PC are the phosphate and the methylated nitrogen moieties. In the phosphate group, the phosphorus has a charge of +1.8 electronic units, the two oxygens sharing the double bond each have a charge of −0.87, and the remaining two oxygens each have −0.65. In the quaternary ammonium group, the nitrogen has a charge of +0.2 and the three methyl groups each have a net charge of +0.13. The most highly charged groups on PS are the phosphate, amino, and terminal carboxyl moieties. In the phosphate group, the phosphorus has a charge of +1.8, the two oxygens sharing the double bond each have a charge of −0.88, and the remaining two oxygens each have −0.69. In the amino group, the nitrogen has a charge of −0.4, and its three hydrogens each have +0.29. In the carboxyl group, the carbon has a charge of +0.76 and the oxygens each have −0.67. The other major charge centers are the carbonyls at the head of each acyl tail: the double-bonded oxygen has −0.58, the single-bonded oxygen has −0.56, and the carbon has +0.9 (Charifson et al., 1990, Table III).

We could find no published data on the charge distributions for PG. We arrived at charges along the fatty acids, the glycerol backbone, and the phosphate on PG by averaging the PS and PC partial charges of Charifson et al. (1990). Charges in the glycerol headgroup were derived using the following rationale. Each of the two —OH groups was given an electric dipole of 0.45 units with a bias toward the oxygen (H = +0.2, O = −0.25). We assigned the remaining charge required to bring PG to a net charge of −1.0 to the headgroup glycerol carbon esterified to the phosphate (C = +0.265). This is comparable to the value estimated for the same atom in PS and PC. All other atoms in the glycerol headgroup were left uncharged.

We also used partial charges calculated by Peinel (1975) after scaling them to the correct net charges for PS (−1) and PC (0). This scaled charge set gave essentially the same result for the potential in the aqueous phase as the charge set for PC:PS model membranes given by Charifson et al. (1990) (results not shown).

Ideal models

We examined several idealized models to determine how the potential adjacent to our model bilayers is affected by the distributed charge, the noncoplanar nature of the charge, the ion-exclusion layer's dielectric constant, and the bumpy surface. We first considered a smooth $\epsilon_r = 2$ slab with hexagonally packed monovalent point charges on its surface. The point charge densities of the slabs are the same as those used for our bilayers: 1 *e*/68 Å^2 (100% PS), 1 *e*/272 Å^2 (25% PS), and 1 *e*/618 Å^2 (11% PS). The slab has a surface area of 130 Å × 116 Å and is 60 Å thick. We applied a 2-Å, $\epsilon_r = 80$ ion-exclusion layer to the slab surface. We distributed the charge by breaking each monovalent charge into six partial charges that were distributed hexagonally around the location of the original charge; each partial charge is 2.22 Å from the central point. Next, we studied the effects of non-coplanarity by burying monovalent point charges at different depths within the slab. We also examined the effect of changing the dielectric constant of the ion-exclusion layer from 80 to 2. Finally, we investigated the effect of the bilayer's rough surface on the potentials by placing hexagonally packed hemispheres with radii = 4 Å and $\epsilon_r = 2$ on the surface of the slab; the distance between the centers of nearest neighbor hemispheres is 8.88 Å. Monovalent charges were placed either at the apex of the hemispheres or on the slab between the hemispheres. In all cases, we assumed the aqueous phase ($\epsilon_r = 80$) contains 0.1 M monovalent salt and the slab (with its hemispheres) is impenetrable to salt.

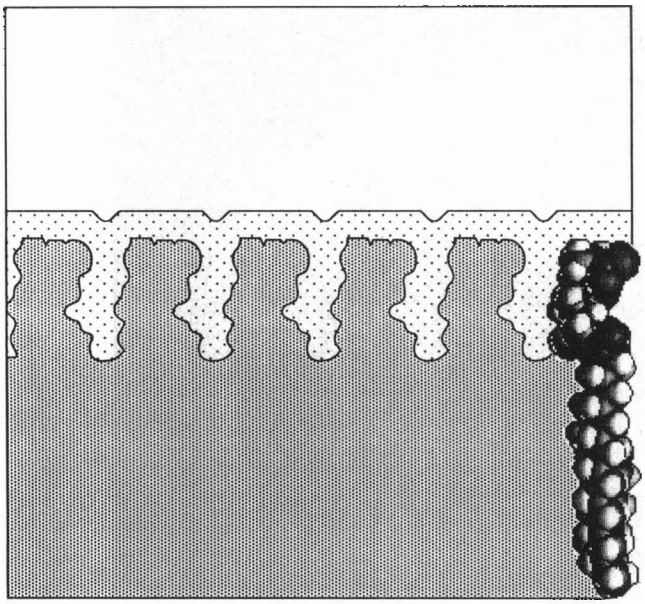

FIGURE 2 Cartoon of a cross-section of the aqueous phase/bilayer interface. The structure of one PS molecule is shown for reference. The aqueous phase (white) has $\epsilon_r = 80$ and contains 0.1 M monovalent salt. The lipids (light gray) have $\epsilon_r = 2$ and are impenetrable to salt. The ion-exclusion layer (stippled region) has $\epsilon_r = 80$ and contains no salt; this region extends 2 Å beyond the lipid atoms into the aqueous phase.

Calculation of electrostatic potentials

We calculated solutions to the nonlinear PB equation using DelPhi, a three-dimensional finite difference program (Gilson et al., 1988; Jayaram et al., 1989; Sharp et al., 1990). A membrane, described in terms of the positions, charges, and radii of its atoms, is mapped onto a 65^3 point cubic lattice. A continuous molecular surface is generated by rolling a spherical probe (1.4 Å radius) over the membrane. The contour traced out by the probe's edge closest to the van der Waals surfaces of the membrane atoms is taken as the molecular surface. The dielectric constant at each lattice point is assigned a value of 2 or 80 depending upon whether it lies inside or outside the molecular surface. The Debye-Hückel parameter ($\kappa = [(2z^2e^2c)/(\epsilon_0\epsilon_r kT)]^{1/2}$ where z is the valence, e the electronic charge, c the number of ions per volume, ϵ_0 the permittivity of free space, and k the Boltzmann constant) has a value of 0 if the lattice point lies within the volume defined by the van der Waals radii of the atoms plus a 2 Å ion-exclusion layer, and has a value of 1/9.6 Å if the lattice point is in the aqueous phase (0.1 M monovalent salt at 25°C). A trilinear interpolation is used to assign charges to the eight lattice sites bounding the volume element in which each atomic charge is located (Klapper et al., 1986). In the initial run, the longest dimension of the membrane comprised only 20% of the lattice dimension (this is referred to as the "% fill"), and we used Debye-Hückel potential boundary conditions (Gilson et al., 1988). At this resolution, the potential at the boundary was 0. For the model phospholipid bilayers, the initial run was followed by three focusing runs (Gilson et al., 1988) at 50, 100, and 200% fill; for each run we used potential values from the previous run to provide the boundary conditions. For the simple ideal models, the initial run was followed by four focusing runs to produce a 400% fill. Periodic boundary conditions were applied in the plane of the membrane for runs at or less than 100% fill. For subsequent runs with a fill >100%, the periodicity is implicitly retained by using the focusing boundary condition. In this way, the calculations simulate an infinite planar membrane. For each run, the potentials were iterated to a convergence of $<10^{-4}$ kT/e potential change between iterations at any lattice point. A further check on convergence is that charge neutrality is satisfied to <1% error.

To speed convergence, we used three-level multigridding with a V cycle, following the approach used by Holst and Saied (1993) for the linear PB equation, combined with the quasi-Newton method for treating the nonlinear portion of the PB equation (Holst et al., 1994). In this method, the finite-difference form of the nonlinear PB is smoothed for several iterations at the finest lattice level (65^3) using the Gauss-Seidel algorithm with a checkerboard updating scheme. The residual, i.e., the amount by which the finite-difference estimate of the nonlinear PB differs from 0 at each lattice point, is then transferred to a coarser grid of 33^3. An estimate of the correction to the potential is computed on the coarser grid, again using a Gauss-Seidel iteration scheme. After several smoothing iterations, the residual is transferred to a still coarser grid of 17^3, and the correction to the potential at that level is solved for by Gauss-Seidel smoothing. After smoothing, the correction from each level is interpolated back into the next finest grid using linear dielectric weighting, and some post-smoothing Gauss-Seidel iterations performed. This cycle is repeated until convergence on the finest grid is achieved.

The dielectric at each coarse lattice point was obtained by harmonically averaging the values at the corresponding two neighbor points on the next finest lattice (Holst and Saied, 1993). The Debye-Hückel parameter at the coarse lattice point was taken directly from the corresponding point in the finer lattice. At least five iterations of smoothing were performed at each level, using a relaxation parameter of 1.2 at the finest mesh and 1.6 on the two coarser meshes.

Convergence generally required 10 cycles of quasi-Newton iteration, lasting about 20 min on a Silicon Graphics Power Station GTX-220 at the lowest resolution, and up to 60 cycles (180 min) at the highest resolution.

Because of the finite resolution of the lattice, errors are introduced when a molecule is mapped onto the lattice. These result from the sensitivity of the electrostatic energy to the exact scale and position of the molecule with respect to the lattice. The dielectric boundary correction technique of Nicholls and Honig (1990) was used to reduce these errors, which were <5% at the final lattice scale of 1 grid/Å or finer.

RESULTS

Bilayers

Fig. 3 shows the potential profiles that we calculated in the aqueous phase adjacent to a model 100% PS bilayer. The potential profiles are essentially planar and do not manifest the structural details of the molecular model apparent in Figs. 1 and 2. Even the −100 mV surface, which is located only about 1 Å from the outermost atoms, is nearly flat. The white tick marks on the right side of Fig. 3 indicate the predictions of Gouy-Chapman theory, which assumes the fixed charge is smeared uniformly over a planar surface. The boundary between our model bilayer and the aqueous phase, however, is not planar (see Fig. 2). To compare our model with the Gouy-Chapman model, we chose the Gouy-Chapman surface (yellow arrow) so that the predicted −100 mV potential matched the one calculated by DelPhi. This results in a Gouy-Chapman surface located immediately adjacent to the outermost atoms in the lipids. With this choice of surface, the other potentials calculated by DelPhi agree well with the predictions of Gouy-Chapman theory.

While discreteness-of-charge effects are absent for the 100% PS bilayer, these effects must appear as the surface charge density of the membrane is lowered. We calculated the equipotential surfaces adjacent to model membranes containing PC/PS mixtures: Fig. 4 shows the −25 mV (1 kT/e at 25°C) profiles for membranes containing 11, 25, or 100% PS. In the 100% PS bilayer, the acidic lipids are 9 Å apart, approximately the Debye length in the aqueous phase, and the equipotential surface is flat (see also Fig. 3). In the 25%

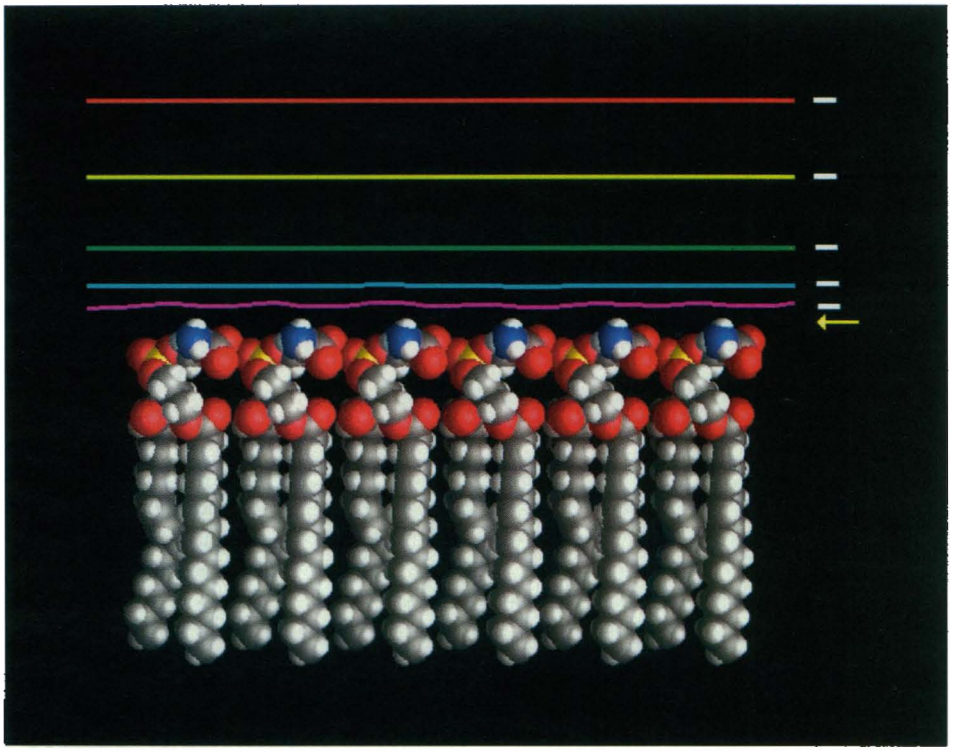

FIGURE 3 Equipotential surfaces in the aqueous phase adjacent to a 100% PS bilayer. The lines show the −12.5 (red), −25 (yellow), −50 (green), −75 (blue), and −100 mV (purple) equipotential surfaces. The aqueous phase contains 0.1 M monovalent salt, T = 25°C. The white tick marks on the right indicate the location of the equipotential surfaces predicted by Gouy-Chapman theory, which assumes the charge is uniformly smeared over a planar surface (yellow arrow).

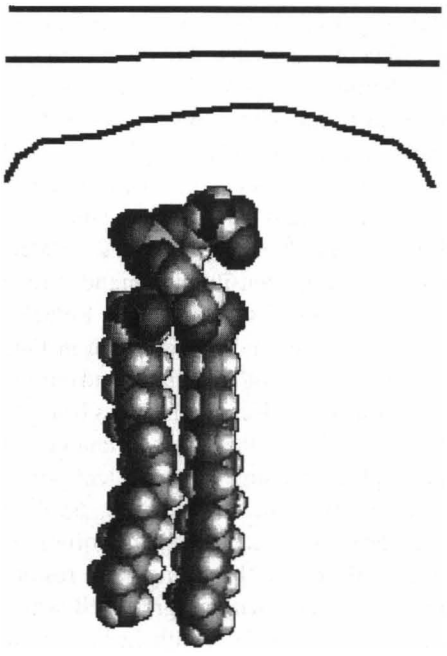

FIGURE 4 The −25 mV equipotential surfaces in the aqueous phase (0.1 M monovalent salt) adjacent to 100, 25, and 11% PS bilayers (top to bottom). A single PS molecule is shown to indicate the position of the bilayer. The equipotential surfaces for the low charge density are discrete domes above the acidic lipids, which are spaced 27 Å apart. The equipotential surfaces for the medium and high charge densities are flat.

PS bilayer, the acidic lipids are 18 Å apart (about twice the Debye length), and there is still sufficient overlap of the potentials from neighboring acidic lipids to produce an equipotential surface that is nearly flat. In the 11% PS bilayer, the acidic lipids are 27 Å apart (three times the Debye length), and the equipotential surface consists of discrete domes. (Calculations using PG in place of PS yielded essentially identical results to those shown above: flat equipotential surfaces for a 100% PG bilayer and discrete surfaces for a <11% PG bilayer.) We obtained the same results when the bilayers contained acidic lipids in only one leaflet or in both leaflets.

Idealized systems

Our simplest model of a membrane is a smooth 60 Å thick, low dielectric (ϵ_r = 2) slab with hexagonally packed monovalent point charges on its surface and a 2 Å thick, high dielectric (ϵ_r = 80) ion-exclusion layer. Fig. 5 *A* shows the −25, −50, −75, and −100 mV equipotential surfaces in the aqueous phase adjacent to a slab with a surface charge density of 1 e/68 Å^2; this charge density corresponds to that of the 100% PS bilayer shown in Fig. 3. Only the −100 mV equipotential surface shows discreteness-of-charge effects (an undulating rather than flat equipotential surface). The other equipotential surfaces are essentially flat. The potentials agree, within calculational error (≤5%), with the potentials predicted by Gouy-Chapman theory (right axis). Appendix I discusses the sources and extent of the errors. At this charge density, the surface potential (the potential at the ion-accessible surface) calculated using Gouy-Chapman theory, which uses the nonlinear PB equation, is much smaller than the surface potential calculated using the linearized PB equation for a smeared charge (−131 mV vs. −327 mV). We obtained similar results with the discrete charges. Experimental results agree with the predictions of Gouy-Chapman theory (McLaughlin, 1977, 1989), demon-

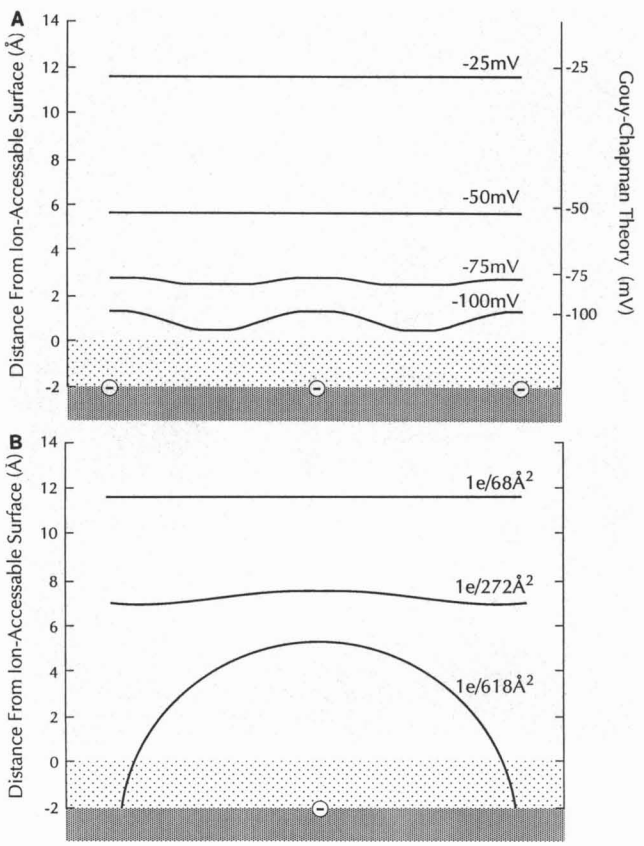

FIGURE 5 (*A*) Equipotential surfaces in the aqueous phase (white) adjacent to a smooth $\epsilon_r = 2$ slab (light gray) with charges packed hexagonally on the surface. The charge density, 1 *e*/68 Å^2, is the same as that for a 100% PS bilayer (Fig. 3). The aqueous phase contains 0.1 M monovalent salt, and the stippled region represents the $\epsilon_r = 80$ ion-exclusion layer. The left axis indicates the distance from the ion-accessible surface. The right ordinate shows the distances predicted by Gouy-Chapman theory. (*B*) The −25 mV equipotential surfaces in the aqueous phase (white) adjacent to smooth $\epsilon_r = 2$ slabs (light gray). The charge densities are the same as for the 100, 25, and 11% PS bilayers. The aqueous phase contains 0.1 M monovalent salt, and the stippled region represents the $\epsilon_r = 80$ ion-exclusion layer. The vertical axis indicates the distance from the ion-accessible surface.

strating the importance of using the nonlinear PB equation to calculate potentials adjacent to membranes with moderate to high charge densities (≥25% acidic lipid). Verwey and Overbeek's (1948) classic text gives a thorough description of the predictions of linear and nonlinear theories for a uniformly charged surface.

Fig. 5 *B* shows how the charge density affects the shape of the potential profiles in the aqueous phase adjacent to the simple slab model of a membrane, illustrating the −25 mV equipotential surfaces for charge densities of 1 *e*/68 Å^2, 1 *e*/272 Å^2, and 1 *e*/618 Å^2. These values correspond to the charge densities of 100, 25, and 11% PS phospholipid model membranes used in Fig. 4. For the lowest charge density, the equipotential profile adjacent to a charge q at the surface closely approximates the profile predicted by Debye-Hückel theory for the potential adjacent to a charge $2q$ in a bulk aqueous solution or the analytical solution to the linearized PB equation for a point charge at the interface between an ion-free $\epsilon_r = 2$ slab and an ion-containing $\epsilon_r = 80$ aqueous phase (Mathias et al., 1992). (If the charge were uniformly smeared, Gouy-Chapman theory predicts that the equipotential surface would be located 2.4 Å away from the ion-accessible surface.) The potential a given distance from a charge is slightly larger than for a single-point charge because of the overlap of the potentials from its neighbors. The equipotential surface for the intermediate charge density is slightly rippled and oscillates about an average that agrees with Gouy-Chapman theory. The equipotential surface for the high charge density is the same as that shown in Fig. 5 *A*.

We also examined the limiting case of low charge density, corresponding to a single point charge on a membrane surface, for the slab model with a 2 Å, $\epsilon_r = 80$, ion-exclusion layer using both the linear and the nonlinear PB equation. The equipotential surfaces are all approximately hemispherical (not shown). The potentials calculated using the linear approximation agreed, within calculational error, with twice Debye-Hückel theory; the factor of 2 arises from the image charge effects (Mathias et al., 1992). The −25 mV equipotential surface calculated using the nonlinear PB equation was within 5% of the surface calculated using the linear approximation, and very close to the potential for the lowest charge density case of Fig. 5 *B*.

The charge on a lipid is not localized on a single atom but is distributed as partial charges over several atoms. We examined the effect of charge distribution in our slab model by replacing each monovalent point charge with six partial (1*e*/6) charges distributed hexagonally around the site of the original charge. Each partial charge is 2.2 Å from the central point. There is little difference between the potentials calculated using distributed charge (not shown) and those shown in Figs. 5, *A* and *B*. As expected, the −100 mV surface for the 1 *e*/68 Å^2 charge density membrane is flatter than in Fig. 5 *A*, and the −25 mV surface for the 1 *e*/618 Å^2 charge density is slightly flatter and broader than in Fig. 5 *B*.

The partial charges on both real lipids and our model phospholipids are located at different distances from the molecular surface. We examined the effect of charge depth in the slab model by placing a single monovalent point charge at different distances from the interface (Fig. 6). As the charge is moved into the slab, the equipotential profiles move closer to the surface and become broader. These results obtained with the nonlinear PB equation agree well with those obtained by Arakelian et al. (1993) with the linearized PB equation. We also buried layers of monovalent point charges (similar to the ones used in Fig. 5 *B*) 2 or 4 Å below the interface. This is the slab model's equivalent of changing the dielectric constant of the bilayer's headgroup region to 2. All the equipotential surfaces for a charge density of 1 *e*/68 Å^2 are flat, are located at the same distances as those shown in Fig. 5 *A*, and agree with the predictions of Gouy-Chapman theory. This independence of the potential in the aqueous phase from the charge ensemble's depth below the slab surface is also observed with a uniformly smeared layer of charge (i.e., Gouy-Chapman theory).

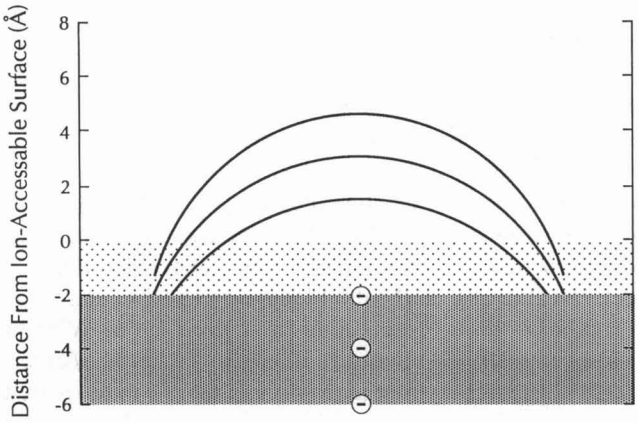

FIGURE 6 The −25 mV equipotential surfaces for a point charge located either at the $\epsilon_r = 2/\epsilon_r = 80$ interface, buried 2 or 4 Å below the slab (light gray) surface. The aqueous phase contains 0.1 M salt and the stippled region represents the $\epsilon_r = 80$ ion-exclusion layer. The vertical axis indicates the distance from the ion-accessible surface. The −25 mV equipotential surface moves closer to the surface and becomes broader as the charge is moved into the slab.

The ion exclusion layer in the slab models above has an $\epsilon_r = 80$; we examined the effect of the dielectric constant in this region by reducing its value from 80 to 2. All other conditions were the same as used in Fig. 5 *B*. There was little difference between the positions of the −25 mV potential contours for each of the three charge densities, although the potential close to the surface charge, of course, is much higher when the ion-exclusion layer has $\epsilon_r = 2$.

Both real bilayers and our model phospholipid membranes have irregular surfaces (e.g., Fig. 2). We examined the effect of surface shape on the potentials by placing hemispheres (4 Å radii) in hexagonal arrays on a slab surface. These hemispheres have $\epsilon_r = 2$ and are impenetrable to the salt ions; they created a bumpy $\epsilon_r = 80$ ion-exclusion layer (stippled region in Fig. 7). We calculated the potentials with the charges placed either at the apex of the hemispheres or on the slab between the hemispheres.

Fig. 7 *A* shows equipotential surfaces where the charges (density = 1*e*/68 Å^2) have been placed at the apex of the hemispheres. The vertical axis shows the distance from the outermost extent of the ion-inaccessible aqueous region (stipple). The equipotential profiles close to the surface follow the contour of the surface: the −100 mV equipotential surface remains ~1 Å from the ion-accessible surface. As the distance from the ion-accessible surface increases, the equipotential surfaces become flatter. In Fig. 7 *B*, we show the charges moved to the other extreme position, at the underlying slab surface between the hemispheres. In this case all of the equipotential surfaces are flat and agree approximately with the predictions of Gouy-Chapman theory. We also saw flat equipotential surfaces when the same density of charges was placed on a flat surface with a 4 Å thick $\epsilon_r = 80$ ion-exclusion layer. Thus for high charge densities the potential profile in the aqueous phase does not depend greatly on the detailed geometry or ϵ_r of the region below the ion-exclusion layer.

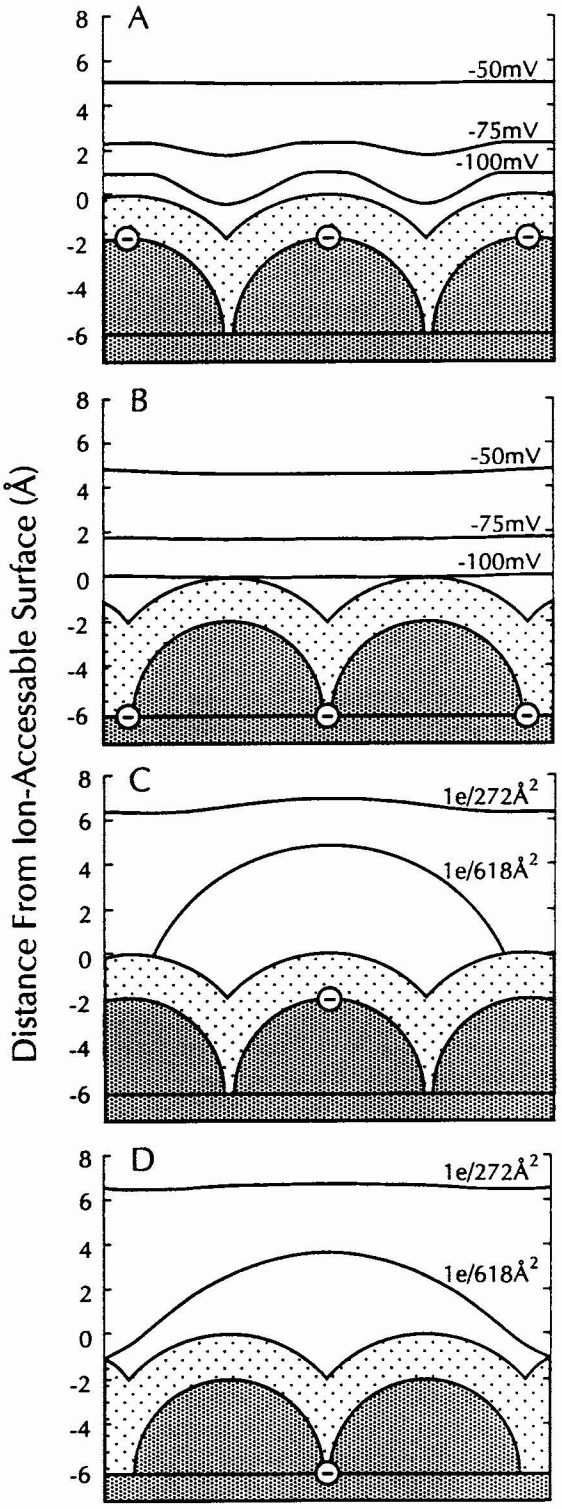

FIGURE 7 Equipotential surfaces in the aqueous phase (white) adjacent to an $\epsilon_r = 2$ slab overlaid with hexagonally packed hemispheres (4 Å radii $\epsilon_r = 2$). The aqueous phase contains 0.1 M salt, and the stippled area represents the $\epsilon_r = 80$ ion-exclusion layer, which reflects the humped shape of the surface. The vertical axis indicates the distance from the outermost extent of the ion-accessible surface. (*A*) and (*B*) show the −50, −75, and −100 mV equipotential surfaces for monovalent point charges (charge density = 1 *e*/68 Å^2) located at the apex and on the slab between the hemispheres, respectively. (*C*) and (*D*) show the −25 mV equipotential surfaces for charge densities of 1 *e*/272 Å^2 (top) and 1 *e*/618 Å^2 (bottom) where the charges are located at the apex and the between the hemispheres, respectively.

Fig. 7, *C* and *D* show the −25 mV equipotential surfaces for charge densities of 1 *e*/272 Å^2 and 1 *e*/618 Å^2. These equipotential surfaces for the 1 *e*/272 Å^2 charge density do not differ significantly from those shown in Fig. 5 *B*. Even the equipotential surface for the 1 *e*/618 Å^2 charge density shown in Fig. 7 *C* is similar to that shown in Fig. 5 *B*.

DISCUSSION AND CONCLUSIONS

The electrostatic potential in the aqueous phase adjacent to model phospholipid bilayers was calculated using the nonlinear PB equation. Membranes containing <11% PS have discrete −25 mV equipotential domes (Fig. 4) that can be approximated using twice Debye-Hückel theory. The equipotential surfaces are clearly not hemispheres, however, because the charge on a lipid is distributed over several atoms. Membranes containing >25% PS have flat −25 mV equipotential surfaces that agree with Gouy-Chapman theory. All the equipotential surfaces adjacent to 100% PS membranes are flat (Fig. 3) and agree with those predicted by Gouy-Chapman theory.

The potentials calculated from our smooth slab model agree well with those calculated for the model phospholipid bilayers. For a slab with a charge density equal to the 11% PS bilayer, the −25 mV equipotential surfaces closely approximate the hemispheres predicted by twice Debye-Hückel theory (Fig. 5 *B*). The equipotential surfaces adjacent to a slab with a point charge density equal to the 100% PS bilayer are approximately flat and agree with the predictions of Gouy-Chapman theory (Fig. 5 *A*).

The four bilayer characteristics we considered (distributed charge, non-coplanar charge, the dielectric constant of the polar headgroup region, and the irregular surface) had little effect on the potentials for moderate or high charge densities. For low charge densities, burying a charge beneath the ion-accessible surface does affect the potentials. The potential profiles in the aqueous phase are drawn closer to the ion-accessible surface and become broader as the charge is buried more deeply within the slab (Fig. 6). When we examined the effect of burying collections of charge at increasing distances from the $\epsilon_r = 2/\epsilon_r = 80$ interface, however, we found the potential profiles in the aqueous phase remained at the same average distance from the membrane and became flatter. For example, the −25 mV contour adjacent to a slab with a medium-to-high charge density is flat and does not change position when the charges are moved further into the slab (not shown). This is because the potential at a particular point has contributions not only from the charge immediately below it, but also from all of the neighboring charges.

In our calculations we modeled the water in both the polar headgroup region and the diffuse double layer as a homogeneous dielectric continuum with $\epsilon_r = 80$. Any attempt to calculate the potential within the polar headgroup region will require a more realistic model for the water molecules in this region. For example, recent experimental (Gawrisch et al., 1992) and theoretical (Berkowitz and Raghavan, 1991; Raghavan et al., 1992; Zheng and Vanderkooi, 1992; Alper et al., 1993; Wilson and Pohorille, 1994) studies suggest that some of the water molecules within the headgroup region are oriented and contribute to the large positive dipole potential that exists within the membrane, a phenomenon we ignore because the dipole potential does not extend into the aqueous phase adjacent to the membrane (McLaughlin, 1977). We were interested in calculating only the potential in the aqueous diffuse double layer due to the fixed charges on the polar headgroups. This potential, of course, depends on the effective value of ϵ_r in the double layer; experimental studies (Marra, 1986; Evans and Parsegian, 1986; Winiski et al., 1986, 1988; Langner et al., 1990; Kraayenhof et al., 1993) suggest that water in the double layer can be treated as a dielectric continuum with $\epsilon_r = 80$ for electrostatic calculations.

Our main conclusion is that simple analytical approximations can be used to calculate the potentials in the aqueous phase (0.1 M salt) when a membrane contains >25% or <11% acidic lipid. For membranes with high concentrations of acidic lipid, Gouy-Chapman theory provides an accurate description of the potentials. For membranes with low concentrations of acidic lipid, the potentials adjacent to each acidic lipid can be approximated using twice Debye-Hückel theory. For membranes containing >11% but <25% PS, which is the range that approximates the composition of a mammalian cell membrane, the equipotential profiles are neither discrete domes nor flat surfaces, but the average potential can be calculated using Gouy-Chapman theory. For phenomena that depend on local variations in the potential, such as the binding of basic peptides to acidic lipids (Mosior and McLaughlin, 1992b) or the effects of charges adjacent to ion channels in membranes (Jordan, 1987), the nonlinear PB equation must be solved for the specific case.

APPENDIX

The simple smooth $\epsilon_r = 2$ slab model provides a good opportunity to examine the sources of error in DelPhi, because the surface is well defined and there are analytical solutions to both the linear and nonlinear forms of the PB equation when the fixed charge is uniformly smeared over a planar surface. There are two main sources of error: the resolution with which a surface is represented on the lattice and the value of the potential at the boundary of the lattice.

We initially searched for errors by solving the linearized PB equation because the potential, $\phi(x)$, should decay from the ion-accessible surface as a single exponential with a space constant equal to $1/\kappa$, the Debye length: $\phi(x) = \phi(0)\exp(-\kappa x)$. We used a charge density of 1 *e*/68 Å^2 and broke each monovalent point charge into six partial charges. These partial charges are distributed hexagonally around the site of the original charge; smearing out the charge reduces any discreteness-of-charge effects. We solved the linearized PB equation using our standard focusing protocol. We plotted $\ln(\phi(x)/\phi(0))$ vs. x and calculated the slope, which is equal to minus the reciprocal of the decay length. The calculated decay length differed from the Debye length by <1%.

The error resulting from the resolution is determined by the spacing of the grids onto which surfaces are mapped. These surfaces include not only the slab and the ion-exclusion layer, whose positions must be defined as input to the calculation, but also the precise position of the equipotential surfaces. The uncertainty in the resolution, ±½ grid spacing, is greatest at the initial focusing run and smallest after the final run. We estimated the error that results from this uncertainly by calculating the potentials first with

the slab surface on a grid plane and then with the slab surface offset by ½ grid spacing from the grid plane at the final run. The calculated potentials differed by 1–2%.

The most significant error comes from the value of the potential at the boundary of the lattice. DelPhi calculates the potential at a grid point (x,y,z) based on the potentials at the six neighboring grid points. If point (x,y,z) is on the edge of the lattice, then a boundary value must be used in place of the missing neighboring grid points. This leads to the question of what the boundary value should be. One obvious choice is to let the potential at the boundary be 0. Because our models are quite large, we must use a very low resolution in order to have the potential sufficiently close to 0 at the boundary. The focusing technique (Gilson et al., 1988) provides a way around this problem. We start with a very low resolution, which permits use of a well defined value of the potential at the boundary. The results from this initial calculation are used to set the boundary values for the next calculation, which uses a higher resolution. This process continues until the desired resolution is achieved. Comparing the calculated potential at the boundary to the value predicted by Gouy-Chapman theory shows that, although this technique provides a reasonable estimate, it is 2–5% lower than the correct value. This is presumably why the −25 mV potential profile calculated in Fig. 5 *A* is slightly closer to the ion-exclusion surface than the value predicted by Gouy-Chapman theory.

This work was supported by National Institutes of Health grant GM-24971 and NSF grant MCB-91–17526 to S. M., American Cancer Society grant PF-3907 to R. M. P., and NSF grant MCB-92–20477 to K. A. S. We thank B. Honig and A. Nicholls for many valuable discussions.

REFERENCES

Adams, R. J., and T. D. Pollard. 1989. Binding of myosin I to membrane lipids. *Nature*. 340:565–568.

Akutsu, H., and T. Nagamori. 1991. Conformational analysis of the polar head group in phosphatidylcholine bilayers: a structural change induced by cations. *Biochemistry*. 30:4510–4516.

Alper, H. E., D. Bassolino-Klimer, and T. R. Stouch. 1993. The limiting behavior of water hydrating a phospholipid monolayer: a computer simulation study. *J. Chem. Phys.* 99:5547–5559.

Arakelian, V. B., D. Walther, and E. Donath. 1993. Electric potential distributions around discrete charges in a dielectric membrane-electrolyte solution system. *Colloid Polym. Sci.* 270:268–276.

Ashcroft, R. G., H. G. L. Coster, and J. R. Smith. 1981. The molecular organisation of bimolecular lipid membranes. The dielectric structure of the hydrophilic/hydrophobic interface. *Biochim. Biophys. Acta*. 643:191–204.

Berkowitz, M. L., and K. Raghavan. 1991. Computer simulation of a water/membrane interface. *Langmuir*. 7:1042–1044.

Bockris, J. O., and A. K. N. Reddy. 1970. Modern Electrochemistry, Vol. 1. Plenum Press, New York.

Büldt, G., H. U. Gally, A. Seelig, and G. Zaccai. 1979. Neutron diffraction studies on phosphatidylcholine model membranes. I. Head group conformation. J. Mol. Biol. 134:673–691.

Buser, C. A., C. Sigal, M. D. Resh, and S. McLaughlin. 1994. Membrane binding of myristoylated peptides corresponding to the NH_2-terminus of Src. *Biochemistry*. 33:13093–13101.

Cevc, G. 1990. Membrane electrostatics. *Biochem. Biophys. Acta*. 1031: 311–382.

Cevc. G., and D. Marsh. 1987. Phospholipid Bilayers. John Wiley and Sons, New York.

Chandler, W. K., A. L. Hodgkin, and H. Meves. 1965. The effect of changing the internal solution on sodium inactivation and related phenomena in giant axons. *J. Physiol.* 180:821–836.

Charifson, P. S., R. G. Hiskey, and L. G. Pedersen. 1990. Construction and molecular modeling of phospholipid surfaces. *J. Comp. Chem.* 11:1181–1186.

Davis, M. E., and J. A. McCammon. 1990. Electrostatics in biomolecular structure and dynamics. *Chem. Rev.* 90:509–521.

de Kruijff, B., A. Rietveld, N. Telders, and B. Vaandrager. 1985. Molecular aspects of the bilayer stabilization induced by poly(L-lysines) of varying size in cardiolipin liposomes. *Biochim. Biophys. Acta*. 820:295–304.

Dilger, J. P., and R. Benz. 1985. Optical and electrical properties of thin monoolein lipid bilayers. *J. Membr. Biol.* 85:181–189.

Evans, E. A., and V. A. Parsegian. 1986. Thermal-mechanical fluctuations enhance repulsion between bimolecular layers. *Proc. Natl. Acad. Sci. USA*. 83:7132–7136.

Fettiplace, R., D. M. Andrews, and D. A. Haydon. 1971. The thickness, composition and structure of some lipid bilayers and natural membranes. *J. Membr. Biol.* 5:277–296.

Forsten, K. E., R. E. Kozack, D. A. Lauffenburger, and S. Subramaniam. 1994. Numerical solution of the nonlinear Poisson-Boltzmann equation for a membrane-electrolyte system. *J. Phys. Chem.* 98:5580–5586.

Gawrisch, K., D. Ruston, J. Zimmerberg, V. A. Parsegian, R. P. Rand, and N. Fuller. 1992. Membrane dipole potentials, hydration forces, and the ordering of water at membrane surfaces. *Biophys. J.* 61:1213–1223.

Gilson, M., K. A. Sharp, and B. Honig. 1988. Calculating the electrostatic potential of molecules in solution: method and error assessment. *J. Comp. Chem.* 9:327–335.

Grahame, D. C. 1958. Discreteness-of-charge-effects in the inner region of the electrical double layer. *Z. Elektrochem.* 62:264–274.

Hancock, J. F., H. Paterson, and C. J. Marshall. 1990. A polybasic domain or palmitoylation is required in addition to the CAAX motif to localize $p21^{ras}$ to the plasma membrane. *Cell*. 63:133–139.

Hauser, H., I. Pascher, R. H. Pearson, and S. Sundell. 1981. Preferred conformation and molecular packing of phosphatidylethanolamine and phosphatidylcholine. *Biochim. Biophys. Acta*. 650:21–51.

Holst, M. 1993. Numerical solutions to the finite-difference Poisson-Boltzmann equation. Ph.D. Thesis. University of Illinois.

Holst, M., R. E. Kozack, F. Saied, and S. Subramaniam. 1994. Protein electrostatics—rapid multigrade-based Newton algorithm for solution of the full nonlinear Poisson-Boltzmann equation. *J. Biomol. Struct. Dynam.* 11:1437–1445.

Honig, B. H., W. L. Hubbell, and R. F. Flewelling. 1986. Electrostatic interactions in membranes and proteins. *Annu. Rev. Biophys. Biophys. Chem.* 15:163–193.

Israelachvili, J. N. 1991. Intermolecular and Surface Forces. Academic Press, New York.

Jayaram, B., K. A. Sharp, and B. Honig. 1989. The electrostatic potential of B-DNA. *Biopolymers*. 28:975–993.

Jordan, P. C. 1987. How pore mouth charge distributions alter the permeability of transmembrane ionic channels. *Biophys. J.* 51:297–311.

Kim, J., P. J. Blackshear, J. D. Johnson, and S. McLaughlin. 1994. Phosphorylation reverses the membrane association of peptides that correspond to the basic domains of MARCKS and neuromodulin. *Biophys. J.* 67:227–237.

Kim, J., M. Mosior, L. Chung, H. Wu, and S. McLaughlin. 1991. Binding of peptides with basic residues to membranes containing acidic phospholipids. *Biophys. J.* 60:135–148.

Klapper, I., R. Hagstrom, R. Fine, K. Sharp, and B. Honig. 1986. Focusing of electric fields in the active site of Cu-Zn superoxide dismutase: effects of ionic strength and amino-acid modification. *Proteins*. 1:47–59.

Kraayenhof, R., G. J. Sterk, and H. W. Wong Fong Sang. 1993. Probing biomembrane interfacial potential and pH profiles with a new type of float-like fluorophores positioned at varying distance from the membrane surface. *Biochemistry*. 32:10057–10066.

Lakhdar-Ghazal, F., J.-L. Tichadou, and J.-F. Tocanne. 1983. Effect of pH and monovalent cations on the ionization state of phosphatidylglycerol in monolayers. *Eur. J. Biochem.* 134:531–537.

Langner, M., D. Cafiso, S. Marcelja, and S. McLaughlin. 1990. Electrostatics of phosphoinisitide bilayer membranes. *Biophys. J.* 57:335–349.

Levine, S. 1971. Adsorption isotherms in the electrical double layer and the discreteness-of-charge effect. *J. Colloid Interface Sci.* 37:619–634.

Li, D., M. Miller, and P. D. Chantler. 1994. Association of a cellular myosin II with anionic phospholipids and the neuronal plasma membrane. *Proc. Natl. Acad. Sci. USA*. 91:853–857.

Magee, A. I., C. M. Newman, T. Giannakouros, J. F. Hancock, E. Fawell, and J. Armstrong. 1992. Lipid modifications and function of the ras superfamily of proteins. *Biochem. Soc. Trans.* 20:497–499.

Marra, J. 1986. Direct measurement of the interaction between phosphatidylglycerol bilayers in aqueous electrolyte solutions. *Biophys. J.* 50:815–825.

Mathias, R. T., G. J. Baldo, K. Manivannan, and S. McLaughlin. 1992. Discrete charges on biological membranes. *In* Electrified Interfaces in Physics, Chemistry, and Biology. R. Guidelli, editor. Kluwer Academic Publishers, The Netherlands. 473–490.

Matthew, J. B. 1985. Electrostatic effects in proteins. *Annu. Rev. Biophys. Biophys. Chem.* 14:387–417.

McDonald, R. C., and A. D. Bangham. 1972. Comparison of double layer potentials in lipid monolayers and lipid bilayer membranes. *J. Membr. Biol.* 9:361–372.

McIntosh, T. J., A. D. Magid, and S. A. Simon. 1989. Range of the solvation pressure between lipid membranes: dependence on the packing density. *Biochemistry.* 28:7904–7912.

McLaughlin, S. 1977. Electrostatic potentials at membrane-solution interfaces. *Curr. Top. Membr. Transp.* 9:71–144.

McLaughlin, S. 1989. The electrostatic properties of membranes. *Annu. Rev. Biophys. Biophys. Chem.* 18:113–136.

McLaughlin, S., and H. Harary. 1976. The hydrophobic adsorption of charged molecules to bilayer membranes: a test of the applicability of the Stern equation. *Biochemistry.* 15:1941–1948.

Mosior, M., and S. McLaughlin. 1991. Peptides that mimic the pseudosubstrate region of protein kinase C bind to acidic lipids in membranes. *Biophys. J.* 60:149–159.

Mosior, M., and S. McLaughlin. 1992a. Binding of basic peptides to acidic lipids in membranes: effects of inserting alanine(s) between basic residues. *Biochemistry.* 31:1767–1773.

Mosior, M., and S. McLaughlin. 1992b. Electrostatics and reduction of dimensionality produce apparent cooperativity when basic peptides bind to acidic lipids in membranes. *Biochim. Biophys. Acta.* 1105: 185–187.

Nelson, A. P., P. Colonomos, and D. A. McQuarrie. 1975. Electrostatic coupling across a membrane with titratable surface groups. *J. Theor. Biol.* 50:317–325.

Nelson, A. P., and D. A. McQuarrie. 1975. The effect of discrete charges on the electrical properties of a membrane. *J. Theor. Biol.* 55:13–27.

Newton, A. C. 1993. Interaction of proteins with lipid headgroups: lessons from protein kinase C. *Annu. Rev. Biophys. Biomol. Struct.* 22:1–25.

Nicholls, A., and B. Honig. 1990. A rapid finite difference algorithm utilizing successive over-relaxation to solve the P-B equation. *J. Comp. Chem.* 12:435–445.

Pearson, R. H., and I. Pascher. 1979. The molecular structure of lecithin dihydrate. *Nature.* 281:499–501.

Peinel, G. 1975. Quantum-chemical and empirical calculations on phospholipids. *Chem. Phys. Lipids.* 14:268–273.

Pollard, T. D., S. K. Doberstein, and H. G. Zot. 1991. Myosin-I. *Annu. Rev. Physiol.* 53:653–681.

Raghavan, K., M. R. Reddy, and M. L. Berkowitz. 1992. A molecular dynamics study of the structure and dynamics of water between dilauroylphosphatidylethanolamine bilayers. *Langmuir.* 8:233–240.

Rand, R. P. 1981. Interacting phospholipid bilayers: measured forces and induced structural changes. *Annu. Rev. Biophys. Bioeng.* 10:277–314.

Sauvé, R., and S. Ohki. 1979. Interactions of divalent cations with negatively charged membrane surfaces. I. Discrete charge potential. *J. Theor. Biol.* 81:157–179.

Scherer, P. G., and J. Seelig. 1987. Structure and dynamics of the phosphatidylcholine and the phosphatidylethanolamine head group in L-M fibroblasts as studied by deuterium nuclear magnetic resonance. *EMBO J.* 6:2915–2922.

Seelig, J., P. M. MacDonald, and P. G. Scherer. 1987. Phospholipid head groups as sensors of electric charge in membranes. *Biochemistry.* 26: 7535–7541.

Sharp, K. A. 1994. Electrostatic interactions in macromolecules. *Curr. Opin. Struct. Biol.* 4:234–239.

Sharp, K. A., and B. Honig. 1990. Electrostatic interactions in macromolecules: theory and applications. *Annu. Rev. Biophys. Biophys. Chem.* 19: 301–323.

Sharp, K. A., A. Nicholls, and B. Honig. 1990. DelPhi: A macromolecular electrostatics software package. Department of Biochemistry and Biophysics, Columbia University, New York.

Shipley, G. G. 1973. Recent x-ray diffraction studies of biological membranes and membrane components. *In* Biological Membranes. D. Chapman and D. F. H. Wallach, editors. Academic Press, New York. 2:1–89.

Simon, S. A., and T. A. McIntosh. 1989. Magnitude of the solvation pressure depends on dipole potential. *Proc. Natl. Acad. Sci. USA.* 86:9263–9267.

Stouch, T. R. 1993. Lipid membrane structure and dynamics studied by all-atom molecular dynamics simulations of hydrated phospholipid bilayers. *Mol. Simulation.* 10:335–362.

Stouch, T. R., and D. E. Williams. 1992. Conformational dependence of electrostatic potential derived charge of a lipid headgroup: glycerylphosphorylcholine. *J. Comp. Chem.* 13:622–632.

Taniguchi, H., and S. Manenti. 1993. Interaction of myristoylated alanine-rich protein kinase C substrate (MARCKS) with membrane phospholipids. *J. Biol. Chem.* 268:9960–9963.

Verwey, E. J. W., and J. Th. G. Overbeek. 1948. Theory of the Stability of Lyophobic Colloids. Elsevier Publishing Co., Inc., New York.

Wiener, M. C., and S. H. White. 1992. Structure of a fluid dioleoylphosphatidylcholine bilayer determined by joint refinement of x-ray and neutron diffraction data. III. Complete structure. *Biophys. J.* 61:434–447.

Wilson, M. A., and A. Pohorille. 1994. Molecular dynamics study of a water-lipid bilayer interface. *J. Am. Chem. Soc.* 116:1490–1501.

Winiski, A. P., M. Eisenberg, M. Langner, and S. McLaughlin. 1988. Fluorescent probes of electrostatic potential 1 nm from the membrane surface. *Biochemistry.* 27:386–392.

Winiski, A. P., A. C. McLaughlin, R. V. McDaniel, M. Eisenberg, and S. McLaughlin. 1986. An experimental test of the discreteness-of-charge effect in positive and negative lipid bilayers. *Biochemistry.* 25:8206–8214.

Zheng, C., and G. Vanderkooi. 1992. Molecular origin of the internal dipole potential in lipid bilayers: calculation of the electrostatic potential. *Biophys. J.* 63:935–941.